Stabilizing Ryanodine Receptors Improves Left Ventricular Function in Juvenile Dogs With Duchenne Muscular Dystrophy

Olivier Cazorla, Inès Barthélémy, Jin Bo Su, Albano C Meli, Valérie Chetboul, Valérie Scheuermann, Vassiliky Gouni, Camille Anglerot, Sylvain Richard, Stéphane Blot, et al.

Stabilizing Ryanodine Receptors Improves Left Ventricular Function in Juvenile Dogs With Duchenne Muscular Dystrophy

Olivier Cazorla, PhD,[a] Inès Barthélémy, VMD-PhD,[b,c] Jin Bo Su, PhD,[b,c] Albano C. Meli, PhD,[a] Valérie Chetboul, VMD-PhD,[b,c] Valérie Scheuermann, MSc,[a] Vassiliky Gouni, VMD-PhD,[b,c] Camille Anglerot, MSc,[a] Sylvain Richard, PhD,[a] Stéphane Blot, VMD-PhD,[b,c] Bijan Ghaleh, PhD,[b,c,*] Alain Lacampagne, PhD[a,*]

ABSTRACT

BACKGROUND Duchenne muscular dystrophy is associated with progressive deterioration in left ventricular (LV) function. The golden retriever muscular dystrophy (GRMD) dog model recapitulates the pathology and clinical manifestations of Duchenne muscular dystrophy. Importantly, they develop progressive LV dysfunction starting at early age.

OBJECTIVES The authors tested the cardioprotective effect of chronic administration of the ARM036, a small molecule that stabilizes the closed conformation of the cardiac sarcoplasmic reticulum ryanodine receptor/calcium release channel (RyR2) in young GRMD-dogs.

METHODS Two-month-old GRMD-dogs were treated with ARM036 or placebo for 4 months. Healthy-dogs of the same genetic background served as controls. Cardiac function was evaluated by conventional and 2-dimensional speckle-tracking echocardiography. Cardiac cellular and molecular analyses were performed at 6 months old.

RESULTS Conventional echocardiography showed normal LV dimensions and ejection fraction in 6-month-old GRMD dogs. Interestingly, 2-dimensional speckle-tracking echocardiography revealed decreased global longitudinal strain and the presence of hypokinetic segments in placebo-treated GRMD dogs. Single-channel measurements revealed higher RyR2 open probability at low resting Ca^{2+} in GRMD cardiomyocytes than in controls. ARM036 prevented those in vivo and in vitro dysfunctions in GRMD dogs. Myofilament Ca^{2+}-sensitivity was increased in permeabilized GRMD cardiomyocytes at short sarcomere length. ARM036 had no effect on this parameter. Cross-bridge cycling kinetics were altered in GRMD myocytes and recovered with ARM036 treatment, which coincided with the level of myosin binding protein-C-S glutathionylation.

CONCLUSIONS GRMD-dogs exhibit early LV dysfunction associated with altered myofilament contractile properties. These abnormalities were prevented pharmacologically by stabilizing RyR2 with ARM036.

Duchenne muscular dystrophy (DMD) affects 1 in 3,500 newborn males and leads to death from respiratory or cardiac failure by the age of 30 years. The cardiac phenotype in DMD patients varies with age ranging from normal left ventricular (LV) structure or function to early onset of dilated cardiomyopathy with heart failure (HF) (1). Presymptomatic cardiac dysfunction is found

From the [a]Phymedexp INSERM, CNRS, Université de Montpellier, CHRU Montpellier, France; [b]Univ Paris Est Creteil, INSERM, IMRB, Creteil, France; and [c]EnvA, IMRB, Maisons-Alfort, France. *Drs Lacampagne and Ghaleh contributed equally and are considered joint senior authors for this work.

The authors attest they are in compliance with human studies committees and animal welfare regulations of the authors' institutions and Food and Drug Administration guidelines, including patient consent where appropriate. For more information, visit the Author Center.

ABBREVIATIONS AND ACRONYMS

DMD = Duchenne muscular dystrophy

Endo = subendocardium

Epi = subepicardium

GRMD = golden retriever muscular dystrophy

HF = heart failure

LDA = length-dependent activation

RyR2 = type 2 ryanodine receptor

SR = sarcoplasmic reticulum

STE = speckle-tracking echocardiography

TDI = tissue Doppler imaging

in 25% of patients younger than 6 years of age increasing to 59% at 10 years. Cardiomyopathy is first clinically evident after 10 years of age and its incidence increases with age, being present in all patients older than 18 years of age (2). There is currently no cure for DMD and established small molecule therapy is limited to reducing the symptoms and hindering the mechanisms of disease progression in the heart. A recent study showed that prophylactic angiotensin-converting enzyme inhibitor treatment in DMD was associated with a significantly higher overall survival and lower rates of hospitalization for HF (3). Thus, there is a need for therapeutic strategies to delay the onset of cardiomyopathy.

Dystrophin deficiency leads to abnormal intracellular calcium (Ca^{2+}) homeostasis in both cardiac and skeletal muscles, which has been proposed to promote the functional muscular abnormalities in DMD patients (4). Consistently, *mdx* mice that completely lack dystrophin exhibit diastolic Ca^{2+} leak from the sarcoplasmic reticulum (SR) due to progressive nitrosylation of the ryanodine receptor/calcium release channel (RyR2) and depletion of FKBP12.6 that likely contributes to the triggering of cardiac arrhythmias and remodeling in DMD (5). Inhibiting the depletion of FKBP12.6 from the RyR2 complex with the Ca^{2+} channel stabilizer S107 (Rycal) stops the SR Ca^{2+} leak, controls aberrant depolarization in isolated cardiomyocytes, and prevents arrhythmias in vivo in *mdx* mice (5).

The RyR2 is emerging as an interesting therapeutic target for improving cardiomyopathy treatment. JTV519, a 1,4-benzothiazepine, was one of the first compounds that restored abnormal RyR function and preserved contractile performance in HF models by enhancing the FKBP12.6 binding to RyR2 (6,7). Derivatives of JTV519 with different RyR specificities have been developed similar to the S107 (8). Another Rycal compound, ARM036 (also known as Aladorian) has been in clinical development for chronic HF To consider targeting RyR2 in DMD patients, a first evaluation in relevant animal models of DMD is required. Unfortunately, *mdx* mice present mild muscle pathology, normal lifespan, and delayed cardiomyopathy when compared with DMD patients due to compensatory mechanisms (9). The golden retriever muscular dystrophy (GRMD) dog model closely mimics the human disease of DMD (10). A mutation in the dystrophin gene of GRMD dogs leads to dystrophic muscle lesions, early locomotor impairment, and premature death due to respiratory or cardiac failure. As in DMD patients, GRMD dogs progressively develop HF with age. We showed in GRMD dogs with HF that cardiomyocytes isolated from the subendocardium (Endo) display marked contractile defaults correlated with abnormal sarcomeric protein phosphorylation and lower endothelial and neuronal nitric oxide synthase content (11). At 6 months of age, cardiac function assessed by conventional echocardiography is similar between GRMD dogs and healthy dogs of the same genetic background (12). However, tissue Doppler imaging (TDI) reveals a decrease in the subendocardial velocity in GRMD dogs before the occurrence of LV dilation and dysfunction analyzed by conventional echocardiography. Recently, we have shown that the speckle-tracking echocardiographic (STE) imaging or 2-dimensional strain was a sensitive technique for detecting myocardial dysfunction before LV ejection fraction depression occurs in pediatric DMD patients and GRMD dogs (13,14). The goal of the present study was to investigate the cardioprotective effects of chronic administration of the ryanodine stabilizer ARM036 at the onset of cardiac dysfunction in young GRMD dogs.

METHODS

ANIMAL MODEL. Experiments were conducted in accordance with the European Parliament Directive 2010/63/EU for the protection of animals used for scientific purposes and were approved by the ethical committee ComEth ANSES-EnvA-UPEC (agreement #11-01-11/06).

A total of 16 GRMD dogs were recruited from the cohort of GRMD dogs of Centre d'Elevage du Domaine des Souches bred (Mézilles, France). The disease was diagnosed by DNA analysis at 1 month of age. This study was a placebo-controlled and a blinded investigation. The 2-month-old GRMD dogs were randomly distributed into the ARM036 group (n = 8) and placebo group (n = 8). The treatment information was blinded to all persons involved in the study. The GRMD dogs of the ARM036 group were administrated with 15 mg/kg ARM036 (provided by ARMGO Pharma and the Institut de Recherches Servier, Cardiovascular Research Unit, and dissolved in saline solution, 50 mg/mL) by gastrostomy tube twice a day for 4 months. This dose was determined by a preliminary pharmacokinetic study. The placebo group was administrated with oral 0.9% sodium chloride (twice

a day) of the same volume as that for the ARM036. At the end of the protocol, GRMD dogs were compared with healthy golden retriever dogs (n = 6) of the same genetic background and age (6 months) that were used as controls.

Muscle biopsy specimens were collected from the tibialis cranialis in 2- and 6-month-old anesthetized dogs and from the left anterolateral free wall, Endo, and subepicardium (Epi), of 6-month-old dogs after sacrifice (pentobarbital, 100 mg/kg). All biopsy specimens were quickly frozen and stored at −80°C until use for ex vivo experiments.

ECHOCARDIOGRAPHY. All conventional and advanced echocardiographic images were acquired using a Vivid 7-dimension system (General Electric Medical System) with 5- to 7.5- and 2- to 5-MHz phased-array transducers in awake (without the use of sedatives and anesthetics) dogs gently restrained in standing posture. Conventional structural and functional parameters, 2-dimensional color TDI images were obtained in accordance with the recommendations of the American Society of Echocardiography.

EX VIVO EXPERIMENTS. RyR2 channel activity was measured from SR vesicles by planar lipid bilayer as described previously (15).

Single permeabilized cardiomyocytes were isolated from the frozen LV myocardial tissues as previously described (16). Myofilament Ca^{2+} sensitivity and cross-bridge cycling kinetics as indexed by the exponential rate of tension redevelopment (k_{tr}) were measured.

STATISTICS. Statistics were performed using StatView 5.0 (SAS Institute). Data are presented as the mean ± SD. Differences were assessed with the 1-way analysis of variance when appropriate. When significant interactions were found, a Holm's post hoc test was applied with $P < 0.05$.

RESULTS

ARM036 IMPROVES IN VIVO LV FUNCTION IN GRMD. The conventional LV functional and structural parameters measured by echocardiography did not differ between the placebo- and ARM036-treated GRMD groups before and after treatment (Table 1). Several parameters increased with age in both groups of GRMD dogs, such as diameter, wall thickness, or functional parameters such as wall thickening (interventricular septum, posterior wall) and Endo and Epi radial systolic velocities. At 6 months of age, the main modification between both GRMD groups and healthy control dogs was a reduction of the transmural gradient of radial myocardial systolic velocity, consistent with previous publications (12,14). ARM036 did not modify this parameter. Interestingly, the myocardial systolic velocity measured by TDI at the mitral annular ring (S_{IVS}) increased with age in ARM036-treated GRMD dogs and not in placebo-treated GRMD dogs (Table 1).

The more sensitive STE detected early changes in LV function. The LV global longitudinal strain (GLS), a systolic function index, was similar between both GRMD groups at 2 months of age (Figure 1C). With aging, the GLS decreased by approximately 10% in placebo-treated GRMD dogs (−20.0 ± 0.9% and −18.1 ± 1.0% in young and adult dogs, respectively). Instead, although not significant, GLS tended to increase by 0.7% in ARM036-treated GRMD-dogs (−20.2 ± 1.0% to −20.9 ± 0.7% in young and adult dogs). At 6 months of age, GLS was lower in placebo-treated

TABLE 1 Body Weight, Heart Rate, and Echocardiographic Data at Baseline and After 4 Months of Treatment

	GRMD + Placebo		GRMD + ARM036		
	Baseline (n = 8)	Placebo (n = 8)	Baseline (n = 8)	+ ARM036 (n = 8)	Healthy Control (n = 6)
Age, mo	1.9 ± 0.2	6.1 ± 0.2	2.1 ± 0.2	6.1 ± 0.1	6.0 ± 0.3
Body weight, kg	3.4 ± 1.4	14.7 ± 3.2[a]	4.2 ± 1.0	16.5 ± 3.8[a]	17.1 ± 3.7
Heart rate, beats/min	181 ± 21	162 ± 26[b]	190 ± 29	153 ± 24[a,b]	122 ± 24
LVEDD, mm	19.6 ± 2.3	31.3 ± 3.7[a,b]	22.2 ± 1.5	34.5 ± 3.3[a]	38.1 ± 6.6
FS, %	39.9 ± 3.2	42.3 ± 4.4[b]	37.9 ± 2.8	39.9 ± 4.6	36.6 ± 2.7
IVSEdT, mm	4.1 ± 1.0	6.4 ± 0.9[a,b]	4.8 ± 0.6	7.3 ± 1.0[a]	8.1 ± 1.6
IVS thickening, %	53.8 ± 16.8	70.1 ± 12.3[a]	55.7 ± 18.2	63.4 ± 16.6	63.1 ± 26.0
LVPWEdT, mm	4.0 ± 0.9	5.9 ± 1.0[a]	4.4 ± 0.5	6.4 ± 0.8[a]	6.7 ± 1.4
LVFW thickening, %	78.4 ± 23.3	78.4 ± 23.5	70.1 ± 10.8	71.0 ± 18.8	68.5 ± 23.2
E, m/s	0.78 ± 0.09	0.91 ± 0.12[a]	0.80 ± 0.10	0.82 ± 0.21	0.81 ± 0.09
A, m/s	0.57 ± 0.12	0.69 ± 0.12	0.62 ± 0.08	0.58 ± 0.14	0.59 ± 0.13
E/A	1.4 ± 0.2	1.4 ± 0.3	1.3 ± 0.3	1.4 ± 0.2	1.4 ± 0.2
$V_{endocardium}$, cm/s	6.3 ± 1.2	8.2 ± 1.3[a]	6.6 ± 1.0	8.1 ± 1.0[a]	8.5 ± 0.8
$V_{epicardium}$, cm/s	3.2 ± 0.9	5.4 ± 0.7[a]	3.8 ± 0.9	5.2 ± 0.9[a]	4.6 ± 0.8
$G_{endo-epi}$, cm/s	3.1 ± 0.8	2.8 ± 0.9[b]	2.8 ± 0.6	2.9 ± 0.6[b]	3.9 ± 0.7
S_{IVS}, cm/s	7.7 ± 0.8	9.2 ± 1.9	7.1 ± 1.3	11.1 ± 1.5[a]	9.9 ± 0.8
E', cm/s	6.6 ± 1.4	9.1 ± 1.0[a]	6.3 ± 0.9	9.5 ± 1.4[a]	8.8 ± 0.6
A', cm/s	4.3 ± 2.0	5.5 ± 1.1	3.8 ± 1.3	5.6 ± 1.0[a]	4.8 ± 0.6
E'/A'	1.69 ± .57	1.78 ± 0.65	1.77 ± 0.47	1.74 ± 0.43	2.07 ± 0.31
E/E'	12.3 ± 3.1	9.9 ± 1.0	13.0 ± 2.4	8.8 ± 3.0[a]	8.7 ± 0.9
EF, Simpson, %	67.1 ± 6.3	60.5 ± 10.0	63.3 ± 5.3	66.1 ± 5.6	64.2 ± 1.3
Hypokinetic segments, number/heart	0.0±0.0	1.6±1.9[a,b]	1.1±1.7	0.1 ± 0.4[c]	0.0 ± 0.0

Values are mean ± SD. [a]Age effect $P < 0.05$ compared with corresponding baseline. [b]Pathology effect $P < 0.05$ compared with healthy control dogs at the same age. [c]Treatment effect $P < 0.05$ compared with the placebo GRMD group at the same age.

A' = A' wave obtained by tissue Doppler imaging at the interventricular septal annulus; E' = E' wave obtained by tissue Doppler imaging at the interventricular septal annulus; EF = ejection fraction; FS = fractional shortening; $G_{endo-epi}$ = gradient of myocardial systolic velocity between the subendocardium and the subepicardium, calculated by subtraction of the radial subepicardial systolic velocity from radial subendocardial systolic velocity; GRMD = golden retriever muscular dystrophy; IVSEdT = interventricular septal wall end-diastolic thickness; IVS = interventricular septal systolic; LVEDD = left ventricular end-diastolic diameter; LVPWEdT = left ventricular posterior wall end-diastolic thickness; LVPW = left ventricular posterior wall systolic; S_{ivs} = myocardial systolic velocity measured by tissue Doppler imaging at the interventricular septal annulus; $V_{endocardium}$ = radial subendocardial systolic velocity; $V_{epicardium}$ = radial subepicardial systolic velocity.

FIGURE 1 **Chronic ARM036-Treatment Reduced Longitudinal Systolic Strain Alterations in GRMD-dogs**

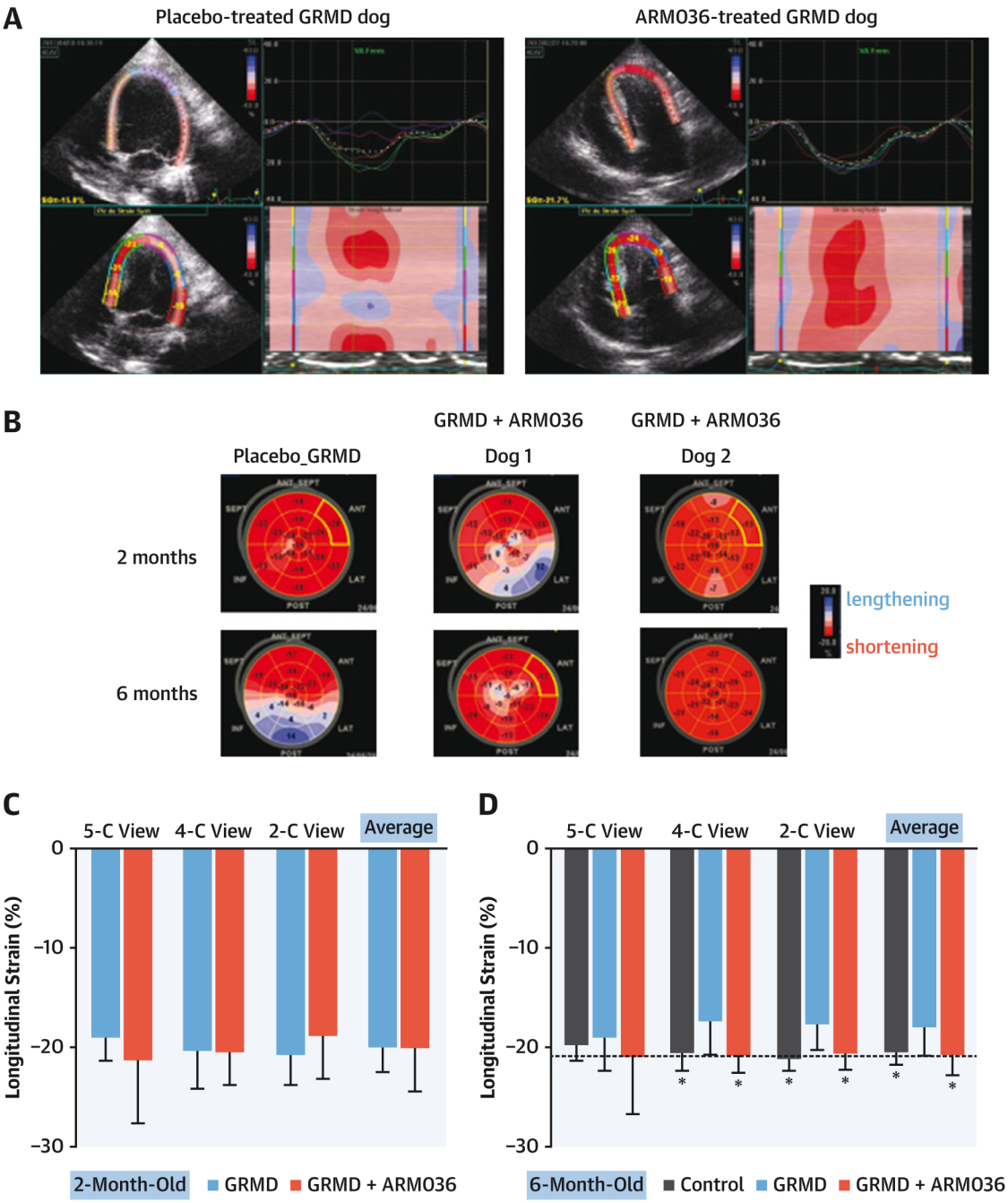

(A) Speckle-tracking analysis of longitudinal strain of a 6-month-old placebo-treated **(left)** golden retriever muscular dystrophy (GRMD) dog reveals 2 dyskinetic segments with heterogeneous time-strain curves. The ARM036-treated GRMD dog **(right)** exhibited normal strain. **(B)** Bulls-eye plot of peak longitudinal systolic strain. After 4 months, the global longitudinal strain (GLS) of the placebo-GRMD dog decreased with the appearance of hypokinetic myocardial segments. The ARM036-treatment improved GLS in both GRMD dogs and reduced the number of hypokinetic segments. **(C, D)** Average GLS obtained from the 3 apical chamber views (5-C, 4-C and 2-C) of GRMD dogs at baseline (2 months of age, **C**) and after placebo (**blue**, n = 8) or ARM036 (**red**, n = 8) treatments (6 months of age, **D**) compared with 6 months of age healthy control dogs (**gray**, n = 6). The **dashed line in D** shows the average GLS at 2 months of age. *$P < 0.05$ versus placebo GRMD.

GRMD dogs compared with healthy control dogs (−20.7 ± 0.5%). ARM036 treatment prevented this reduction in GLS in GRMD dogs. Moreover, placebo-treated GRMD dogs had hypokinetic segments (ie, a strain value >−10%), which were not detected in control and ARM036-treated GRMD dogs (**Figure 1, Table 1**).

The diastolic function was investigated by the E/A and E/E' ratios. The E/A ratio did not differ between placebo-treated and ARM036-treated GRMD dogs. ARM036-treated GRMD dogs showed a greater E' peak and smaller E/E' after 4 months of treatment than at baseline, whereas placebo-treated GRMD dogs had no significant changes in these parameters. The contractile defaults observed in vivo were not associated with cardiac fibrosis (Supplemental Figure 2).

ARM036 PREVENTS FUNCTIONAL AND STRUCTURAL CHANGES OF RyR2 COMPLEX IN GRMD. Intracellular calcium homeostasis impairment in the cardiomyocytes may contribute to any remodeling of the contractile properties of the cardiac tissue. To test this hypothesis, myocardial biopsy specimens were collected from 2 LV regions, Endo and Epi, of all animals. We measured the properties of single RyR2 and its ability to transport the Ca^{2+} by single-channel recordings in planar lipid bilayers (**Figures 2A to 2D**). In both Endo and Epi, the single-channel RyR2 in GRMD opens more frequently as indicated by the higher open probability (Po) in GRMD RyR2 (0.174 ± 0.041 and 0.124 ± 0.036) compared with control RyR2 (0.015 ± 0.015 and 0.026 ± 0.005). ARM036 prevented this increase of Po (0.067 ± 0.022 and 0.030 ± 0.010 for Endo and Epi, respectively). The RyR2 Ca^{2+} leak observed in GRMD may be explained by the dissociation of the stabilizing protein FKBP12.6 from the RyR2 macromolecular complex in both Endo and Epi of GRMD dogs (**Figure 2F**). ARM036 prevented the FKBP12.6 depletion from RyR2 in both tissue layers.

CARDIAC MYOFILAMENT FUNCTION OF GRMD DOGS AND EFFECT OF ARM036. Downstream to the intracellular calcium homeostasis, functional changes of the contractile machinery (ie, sarcomeres) may also account for the in vivo cardiac contractile defaults. Thus, we investigated specifically the contractile machinery properties in myocytes isolated from Endo and Epi biopsy specimens of GRMD and healthy dogs. Myocytes were permeabilized and attached to establish the steady-state $[Ca^{2+}]$-tension relationship at short (1.9 μm) and long sarcomere length (SL) (2.3 μm) to cover the physiological working range (**Figure 3, Table 2**). This protocol examines how length change modulates force production, for example, length-dependent activation (LDA), which supports the cardiac Frank-Starling mechanism (**Figure 3**). Usual parameters describing the steady-state tension-$[Ca^{2+}]$ relationship were similar among placebo-treated and ARM036-treated GRMD groups. In contrast with adult animals, no difference in the contractile parameters was observed between Endo and Epi. All groups had similar maximal Ca^{2+}-activated force (**Figure 3C to 3D**) and cooperativity of thin filament activation indexed by the Hill coefficient (n_H) (**Table 2**). In contrast, in both Endo and Epi of placebo-GRMD and ARM036-GRMD dogs versus control dogs, the calcium concentration at which force is half-maximal (pCa_{50}) was higher at short SL indicating increased myofilament Ca^{2+}-sensitivity (**Figure 3E to 3F**). This suggests that less free Ca^{2+} is required to produce force in GRMD cardiomyocytes. LDA indexed by the average difference between pCa_{50} at long and short SL (ΔpCa_{50}) was lower in GRMD myocytes only in the subendocardial region (**Figure 3G**). ARM036 had no beneficial effect on LDA.

ARM036 PREVENTS ALTERATIONS OF CROSS-BRIDGE PROPERTIES IN GRMD. To further explore the contractile properties, we measured the speed of muscle shortening in permeabilized cardiomyocytes (**Figure 4**). The dynamic contractility was measured either at submaximal or at maximal Ca^{2+}-activation by the rate of tension recovery (K_{tr}) after a rapid shortening/restretch procedure of the myocyte, which allows to estimate the rate of transition from non-force-generating to force-generating cross-bridges (**Figure 4A**). Most of the changes of k_{tr} occurred at short SL (**Figures 4B to 4D**) in both Endo and Epi cells. In both layers, k_{tr} increased at short SL at submaximal Ca^{2+}-activation, and decreased at maximal Ca^{2+} activation in GRMD dogs as compared to healthy control dogs. The alterations of cross-bridge attachment or detachment speeds in GRMD were prevented by ARM036.

POST-TRANSLATIONAL MODIFICATIONS OF THE CONTRACTILE MACHINERY. We examined several molecular mechanisms including sarcomeric protein degradation and post-translational modifications that could explain the changes in the contractile machinery properties induced by the pathology and treatment (**Figure 5 and** Supplemental Table 1). Both cardiac troponin I (cTnI) and cardiac myosin binding protein-C (cMyBP-C) are important modulators of cross-bridge cycling and myofilament Ca^{2+}-sensitivity and are targeted by the ß-adrenergic-activated protein kinase A (17,18).

Degradation of cTnI was not observed in GRMD (**Figure 5A**). cTnI phosphorylation at the protein kinase A–dependent $Ser^{22/23}$ site increased only in Epi

FIGURE 2 The Cardiac RyR2 Macromolecular Complex in GRMD Dogs

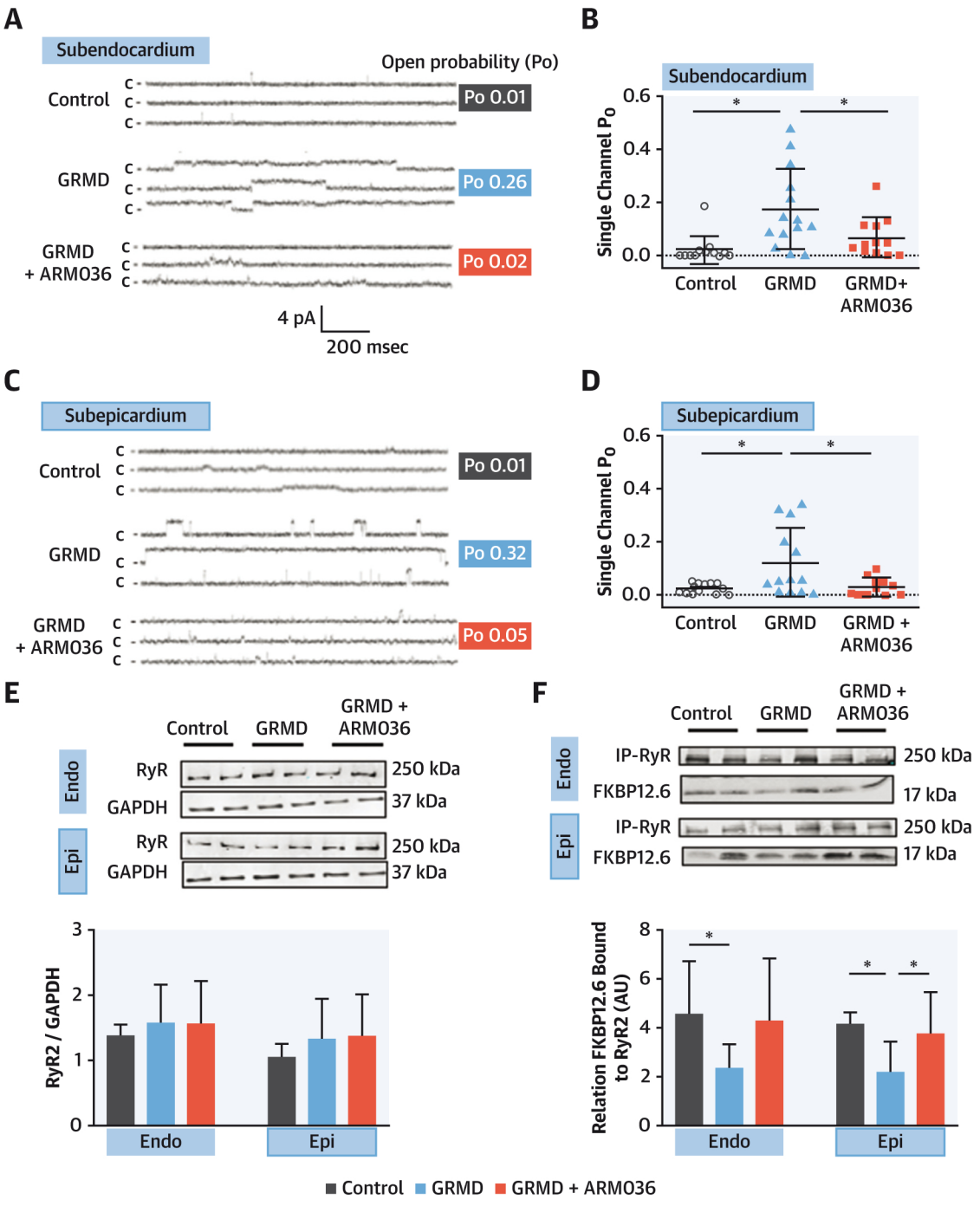

(A to D) Example of RyR2 single-channel activity measurement by planar lipid bilayer technique, isolated from the subendocardium **(A)** and subepicardium **(C)** of healthy control **(gray),** GRMD **(blue),** and GRMD + ARMO36 **(red)** dogs. The label "C" indicates the closed state. Single-channel activity of RyR2 reveals increased open probability (Po) at low diastolic [Ca^{2+}] in subendocardium (Endo) **(B)** and subepicardium (Epi) **(D)** of GRMD dogs (n = 10 to 14 channels from 3 animals in each group). An asterisk (*) indicates $P < 0.05$ versus placebo GRMD. **(E)** Ryanodine receptor/calcium release channel 2 (RyR2) content measured by Western blot analysis in the Endo and Epi of control (**open bar**, n = 4), GRMD (**blue**, n = 8), and GRMD + ARMO36 (**red**, n = 8) dogs. **(F)** Immunoprecipitation of RyR2 and quantification of FKBP12.6 binding by Western blot. *$P < 0.05$ versus placebo-GRMD group. GAPDH = glyceraldehyde 3-phosphate dehydrogenase; other abbreviations as in Figure 1.

TABLE 2 Mechanical Properties of Permeabilized Cardiomyocytes From 6-Month-Old Control, GRMD, and ARM036-Treated GRMD Dogs

	Endo			Epi		
	Control (n = 16/4)	GRMD (n = 31/8)	GRMD + ARM036 (n = 42/8)	Control (n = 16/4)	GRMD (n = 30/8)	GRMD+ARM036 (n = 30/8)
SL short						
pCa_{50}	5.72 ± 0.07	5.82 ± 0.16[a]	5.88 ± 0.14[a]	5.73 ± 0.04	5.81 ± 0.13[a]	5.85 ± 0.15[a]
Hill coefficient, nH	3.4 ± 0.9	3.4 ± 1.2	3.2 ± 1.0	3.6 ± 0.9	3.6 ± 1.2	3.2 ± 0.8
Maximal tension, mN/mm^2	31 ± 12	27 ± 10	26 ± 10	35 ± 13	30 ± 9	33 ± 12
Passive tension, mN/mm^2	1.0 ± 0.9	1.3 ± 1.6	1.8 ± 2.0	0.7 ± 1.0	1.7± 1.5[a]	1.7 ± 1.4[a]
K_{tr} submax, s^{-1}	0.52 ± 0.23	0.94 ± 0.95[a]	0.65 ± 0.32[b]	0.59 ± 0.19	1.06 ± 0.79[a]	0.61 ± 0.25[b]
K_{tr} max, s^{-1}	1.58 ± 0.80	0.97 ± 0.51[a]	1.56 ± 0.55[b]	1.58 ± 0.68	1.11 ± 0.50	1.57 ± 0.52
SL long						
pCa_{50}	5.90 ± 0.10	5.96 ± 0.03	6.02 ± 0.03[a]	5.89 ± 0.07	5.95 ± 0.16	6.02 ± 0.17[a]
Hill coefficient, nH	4.0 ± 1.0	3.4 ± 0.8[a]	3.2 ± 1.0	3.9 ± 0.9	3.4 ± 0.9	3.6 ± 1.0[a]
Maximal tension, mN/mm^2	33 ± 11	31 ± 10	30 ± 10	40 ± 12	33 ± 10[a]	36 ± 13
Passive tension, mN/mm^2	4.0 ± 1.6	6.0 ± 3.4[a]	6.1 ± 4.0	5.1 ± 2.7	7.0 ± 4.2	7.2 ± 4.9
K_{tr} submax, s^{-1}	0.62 ± 0.37	0.79 ± 0.15	0.63 ± 0.28[b]	0.41 ± 0.11	0.66 ± 0.39	0.53 ± 0.30
K_{tr} max, s^{-1}	1.74 ± 0.36	0.81 ± 0.57[a]	1.41 ± 0.45[b]	1.42 ± 0.63	1.15 ± 0.62	1.21 ± 0.35
Delta pCa_{50}	0.18 ± 0.07	0.14 ± 0.15[a]	0.14 ± 0.06[a]	0.16 ± 0.07	0.14 ± 0.06	0.16 ± 0.06

Values are mean ± SD, with the number of cardiomyocytes/hearts given between brackets. Passive tension was measured at pCa 9 and maximal active tension was measured at pCa 4.5. The rate constant of force redevelopment (*k*tr) was measured at pCa 5.875 (submaximal) and pCa 4.5 (maximal). Ca^{2+} sensitivity of force (pCa_{50}) (pCa =-log[Ca^{2+}])and nH values were derived by fitting the force-pCa relationships to the Hill equation. [a]$P < 0.05$ versus healthy control dogs. [b]$P < 0.05$ for comparing GRMD with GRMD + ARM036.

Endo = subendocardium; Epi = subepicardium; pCa_{50} = calcium concentration at which force is half-maximal; SL = sarcomere length; other abbreviations as in Table 1.

tissues of placebo- and ARM036-treated GRMD dogs. The cTnI phosphorylation at the Thr^{143} site has been shown to increase myofilament Ca^{2+}-sensitivity. However, this phosphorylation site was similar in the myocardium of placebo-GRMD dogs and tended to decrease in ARM036 dogs when compared with control dogs (Figure 5B).

cMyBP-C followed the same pattern of expression as cTnI with a slight increase in the Epi tissues of both GRMD groups (Figure 5C). The phosphorylation level of cMyBP-C was similar in all conditions. Moreover, cMyBP-C is a target of S-glutathionylation, a reversible post-translational modification between glutathione and redox-sensitive cysteine, activated during oxidative stress and altering myofilament Ca^{2+}-sensitivity (19-21). Interestingly, the level of S-glutathionylation of cMyBP-C increased in both Endo and Epi in GRMD hearts. These modifications were prevented by ARM036 (Figure 5D).

We also studied the myosin light chain 2 (MLC2) whose phosphorylation increases myofilament Ca^{2+} sensitivity. The pSer20-MLC2 level was unchanged between GRMD and control dogs (Supplemental Figure 3A). Finally, since the myosin heavy chain (MHC) isoforms composition affects the speed of muscle shortening, we quantified the level of ß-MHC that is the major isoform expressed in dogs (Supplemental Figure 2B). The level of ß-MHC increased only the Endo tissues of ARM036-treated GRMD dogs. Altogether, the results indicate slight post-translational modifications of the major regulatory contractile proteins investigated in GRMD hearts. The only preventive effect of ARM036 was observed on the level of S-glutathionylation of cMyBP-C, a reversible redox-sensitive post-translational modification.

SKELETAL MUSCLE FUNCTION. The skeletal function was evaluated to determine whether ARM036, which can also target the skeletal muscle isoform of ryanodine receptor (RyR1), is specifically improving DMD-associated cardiomyopathy or is also improving the muscular phenotype in the model. At treatment initiation, 2-month-old GRMD dogs had clear locomotor impairment, evidenced by increased locomotion disability index relative to normal dogs (Figure 6A). The histopathology index was markedly increased in skeletal muscle, showing early alteration of this tissue (Figure 6B). ARM036 treatment had no detectable effect on histopathology or on the locomotion that aggravated similarly in both groups over the 4-month period.

DISCUSSION

Our study shows with a canine model of DMD that chronic administration of ARM036 delayed the progression of early LV dysfunction by restoring the

FIGURE 3 Mechanical Properties of Cardiomyocytes Isolated From 6-Month-Old Dogs

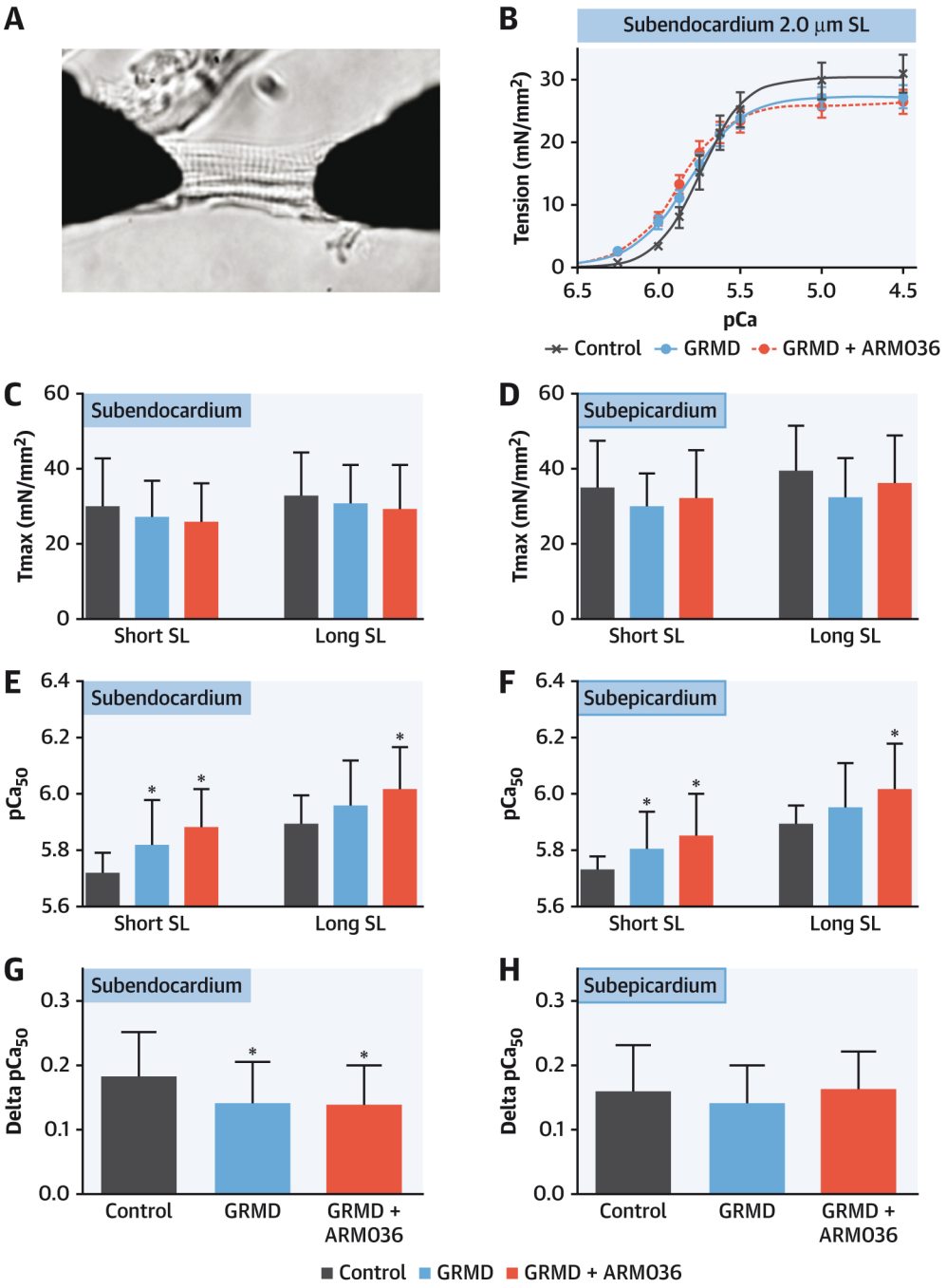

(A) Typical CCD image of a permeabilized cardiomyocyte. **(B)** Example of tension-pCa (=-log[Ca^{2+}]) curves obtained from Endo cardiomyocytes at 2.0 μm sarcomere length (SL) isolated from healthy control **(cross)**, GRMD (**blue circle, line**), and GRMD + ARM036 (**red circle, dashed line**) dogs. The tension-pCa curves were established at short and long SL in permeabilized cardiomyocytes isolated from Endo **(C, E, G)** and Epi **(D, F, H)** layers. **(C-H)** Average contractile parameters of cardiomyocytes isolated from healthy control (**gray bar**, n = 16 cells/4 animals), GRMD (**blue bar**, n = 31 cells/8 animals), and GRMD + ARM036 (**red bar**, n = 30 to 42 cells/8 animals) dogs. Maximal active tension generated in Endo **(C)** and Epi cells **(D)**. Myofilament Ca^{2+}-sensitivity (pCa_{50}) at 2 SL in Endo **(E)** and Epi cells **(F)**. Transmural length-dependent activation (ΔpCa_{50}) in subendocardial **(G)** and subepicardial cells **(H)**. *$P < 0.05$ versus control. CCD = charge coupled device; pCa =-log[Ca^{2+}]; T_{max} = maximal active tension; other abbreviations as in Figures 1 and 2.

FIGURE 4 Cross-Bridge Cycling Kinetics of Cardiomyocytes Isolated From 6-Month-Old Dogs

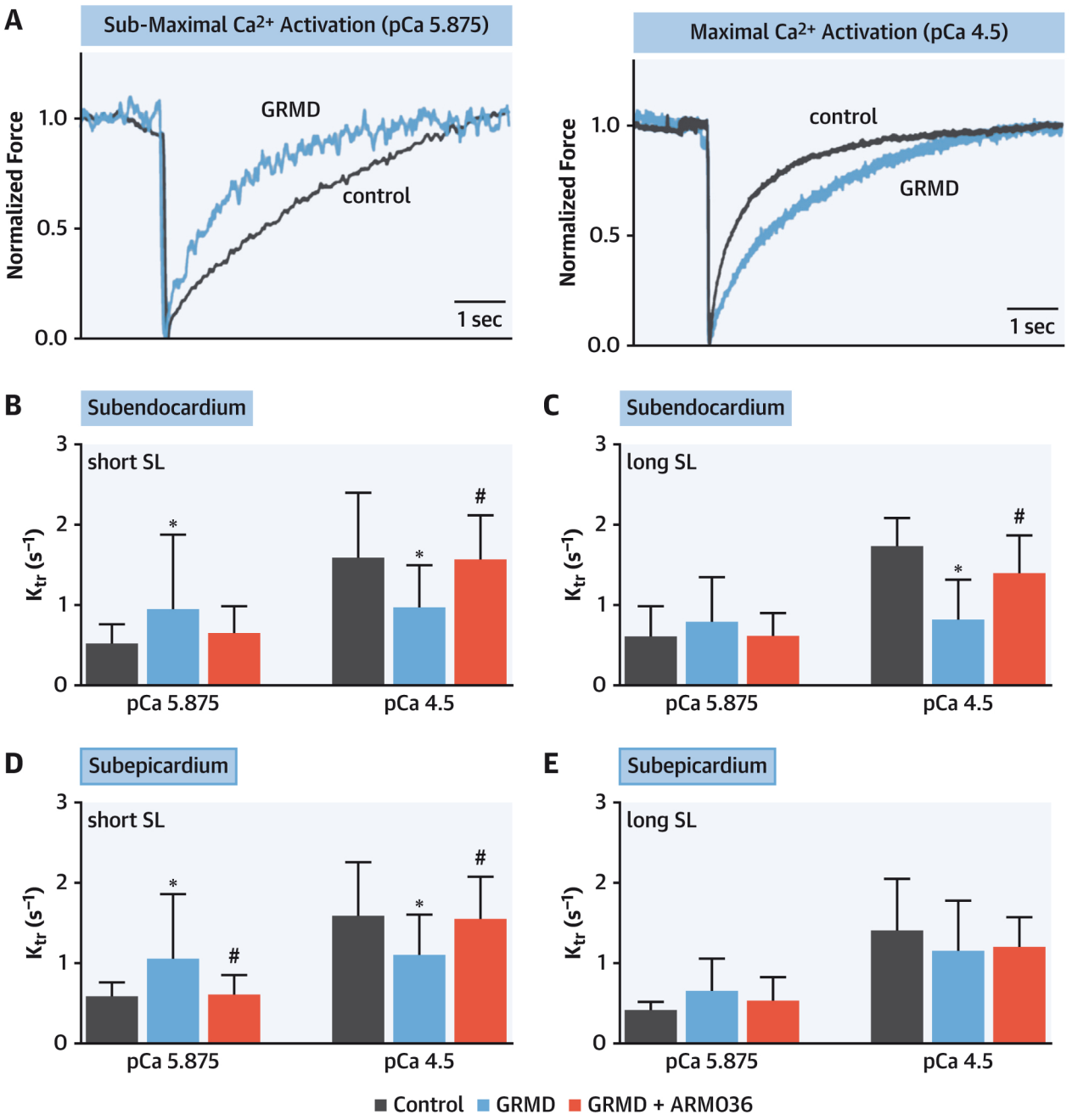

(A) Raw tension recording following rapid muscle length shortening of control **(black trace)** and GRMD **(blue trace)** permeabilized cardiomyocytes at submaximal **(left)** and maximal **(right)** Ca^{2+}-activation. **(B to E)** Average constant of tension redevelopment (K_{tr}) obtained at submaximal [Ca^{2+}] (pCa 5.875) and at maximal [Ca^{2+}] (pCa 4.5) from healthy control **(gray bar),** GRMD **(blue bar)**, and GRMD + ARM036 **(red bar)** cardiomyocytes isolated from Endo **(B, C)** and Epi **(D, E)** at short **(B and D)** and long **(C and E)** SL. N = 3 to 4 cells per animal; GRMD (n = 8), GRMD + ARM036 (n = 8), and control (n = 4). *$P < 0.05$ versus control, and #$P < 0.05$ versus GRMD. Abbreviations as in Figures 1-3.

FIGURE 5 Molecular Remodeling of Regulatory Contractile Proteins in GRMD Dogs

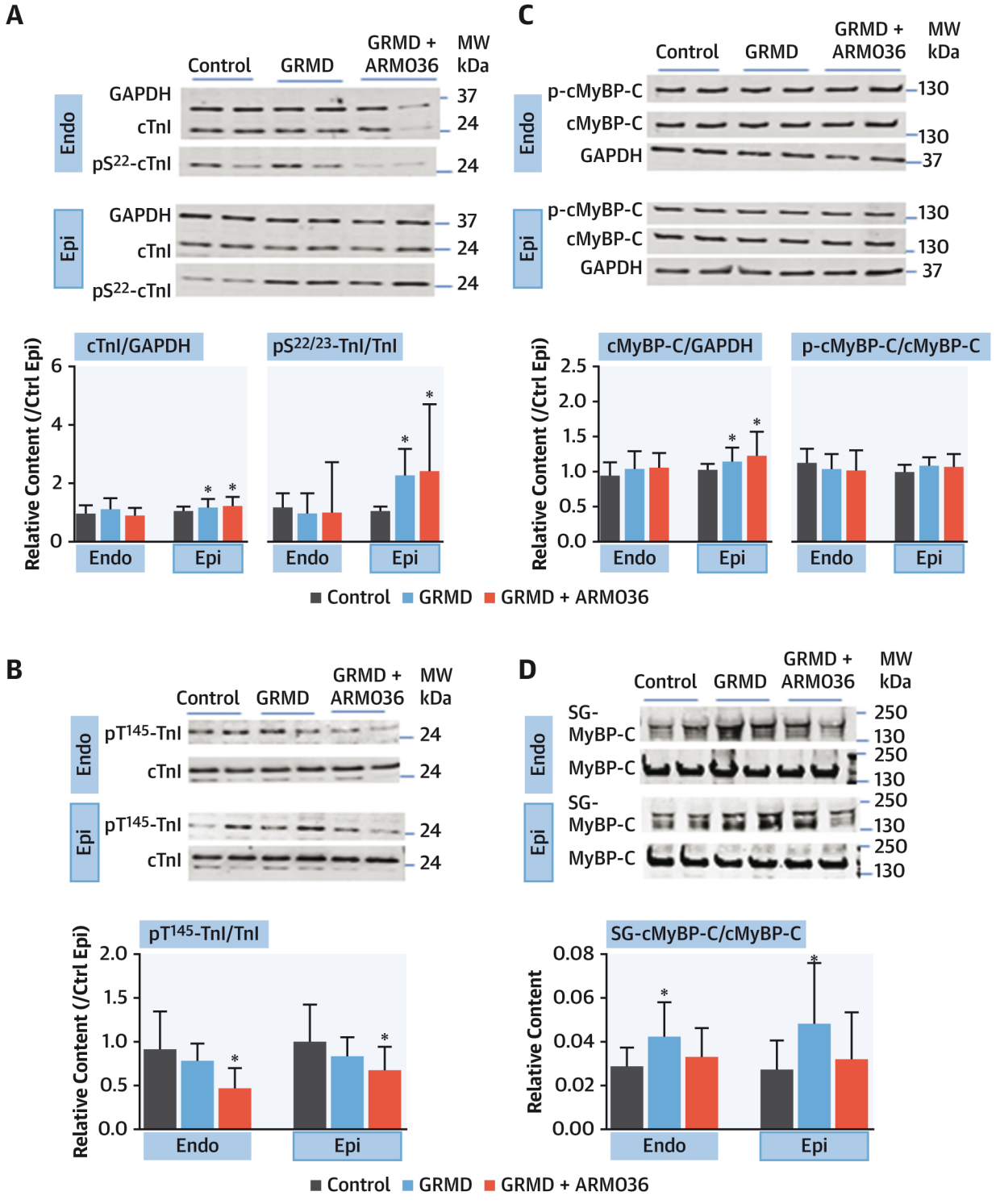

All data are shown for control (**gray bars,** n = 4), GRMD (**blue bars,** n = 8), and GRMD + ARMO36 (**red bars,** n = 8) dogs from Endo and Epi biopsy specimens. **(A, B)** Representative sodium dodecyl sulphate-polyacrylamide gel electrophoresis (SDS-PAGE) and quantification of cardiac troponin I (cTnI) blotted for total cTnI and cTnI-pS$^{22/23}$ **(A)**, and cTnI-pT^{145} **(B)**. **(C, D)** Representative SDS-PAGE and quantification of cardiac myosin binding protein C (cMyBP-C) blotted for total cMyBP-C and cMyBP-C-pS^{282} **(C)** and s-glutathionylation (SG-cMyBP-C) **(D)** (in duplicate). *$P < 0.05$ versus control. GAPDH = glyceraldehyde 3-phosphate dehydrogenase. Antibodies references in Supplemental Table 1. Other abbreviations as in **Figures 1 to 3**.

FIGURE 6 Skeletal Muscle Function and Histopathology

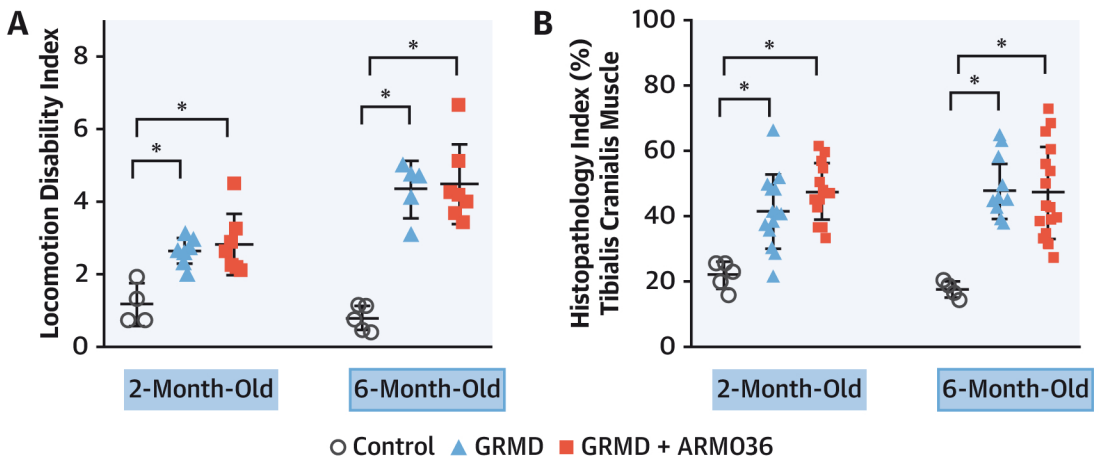

(A) The locomotion disability index quantifies deviation from normal gait according to 7 variables of accelerometry-based gait analysis in control (n = 6), GRMD (n = 8), and GRMD + ARM036 (n = 8) dogs. **(B)** Histopathology index was measured by analyzing hematoxylin and eosin–stained tibialis cranialis muscle biopsy specimens as a percentage of histological events different from normal aspect myofibers. *$P < 0.05$ versus control. Abbreviation as in Figure 1.

normal FKBP12.6-mediated stabilization and closed conformation of the RyR2 (**Central Illustration**).

Therapeutics to treat the dilated cardiomyopathy in DMD patients are limited. Thus, early detection and treatment of cardiac dysfunction is a clinical priority. This prospective randomized and blinded preclinical study examined the effect of stabilizing RyR2 with ARM036 on the evolution of the LV (dys) function in young GRMD dogs. At 6 months of age, placebo-treated GRMD dogs exhibited early signs of LV dysfunction as shown by a decreased transmural gradient of radial systolic velocity and interventricular septum myocardial velocity (S_{IVS}) detected by TDI as well as a worsened longitudinal strain analyzed by STE. This was not associated with cardiac fibrosis that occurs latter (>12 months) with the severity of the cardiomyopathy (11,14). Interestingly, chronic administration of ARM036 in GRMD dogs prevented the alterations in systolic parameters such as S_{IVS} and LV longitudinal strain, and improved diastolic function with a reduced E/E' ratio. This can be explained by its effect on RyR2 to prevent the intracellular Ca^{2+} leak and accumulation during diastole as reported in *mdx* (5). This strongly suggests the link between RyR2 early alteration and progressive cardiac strain dysfunction seen in DMD (13). Our study also shows that the preventive effects of ARM036 on cardiac function are mediated by some effects on the cross-bridges cycling kinetics of the contractile machinery and redox-dependent post-translational modification of the sarcomeric cMyBP-C.

The early LV systolic alterations in GRMD are consistent with previous report showing reduced LV transmural gradient of radial myocardial systolic velocity, LV twist, and GLS very early, at least at 2 months old, compared with control dogs (14). We show here that those changes are associated with cellular and molecular alterations of the components of excitation-contraction coupling involved in the Ca^{2+}-release, namely, the RyR2 and the contractile machinery. The modifications were observed in both the Endo and Epi. The contractile machinery alterations were slightly more pronounced in the Endo at this young age, consistent with the preferential decrease of the endocardial velocity at that age (14). This trend is very likely to increase with age as previously reported in 1-year-old GRMD dogs with reduced LV ejection fraction and subsequent HF (11,22). The altered layer can be preferentially restored by treatments such as moderate exercise training or pharmacological Ca^{2+}-sensitizer and bradykinin associated with improved global function (11,16,23). Surprisingly, the transmural velocity gradient measured by TDI was not reversed by ARM036 treatment. However, this index is closely correlated with myocardial blood flow measured by the microsphere technique (24). ARM036 drug may have limited vasodilator actions; thus, its effect on

CENTRAL ILLUSTRATION Treating Early Cardiac Dysfunction in Dogs With Duchenne Muscular Dystrophy

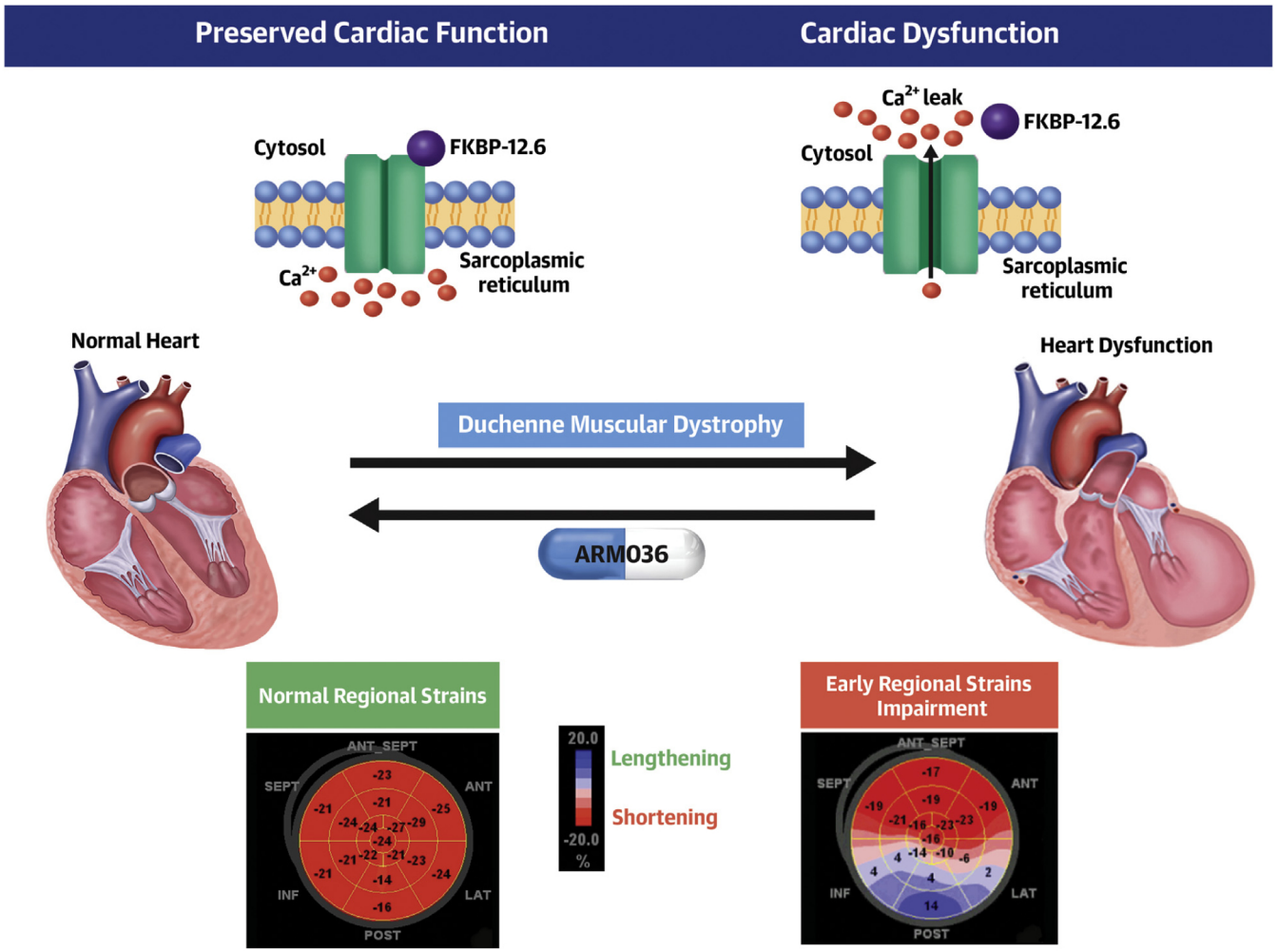

Cazorla, O. et al. J Am Coll Cardiol. 2021;78(24):2439-2453.

The present work is a preclinical prospective study using a large animal model of Duchenne muscular dystrophy (DMD) that identified a phenotype of early cardiac dysfunction caused by abnormal calcium handling and prevented by chronic administration of the ARM036, a small molecule that stabilizes the cardiac sarcoplasmic reticulum ryanodine receptor/calcium release channel (RyRcal) in young golden retriever muscular dystrophy (GRMD) dogs, at the early onset of DMD-related cardiomyopathy.

the index reflecting the myocardial blood flow may not be evident.

The lack of dystrophin induces chronic stress leading to HF in GRMD dogs, tightly associated with changes in regional ultrastructure, post-translational modifications of regulatory proteins, and myofilament contractile properties (11,22). Consistently, increased myofilament Ca^{2+}-sensitivity and reduced phosphorylation levels of cMyBP-C, cTnI, and myosin light chain 2 (MLC-2) have been reported in older dogs with hypertension induced by bilateral renal wrapping, a presumed model of HF with preserved ejection fraction (25). Thus, hypophosphorylation of sarcomeric proteins in large animal models could be a general property in the transition to many HF pathologies. Younger GRMD dogs had also increased myofilament Ca^{2+}-sensitivity but no hypophosphorylation of sarcomeric proteins, suggesting that this may be a secondary mechanism that will occur later. The main post-translational modification of contractile proteins observed in young GRMD dogs was a higher S-glutathionylation of cMyBP-C. Several evidences link myofilament S-glutathionylation and impaired cardiac function. We recently correlated the level of cMyBP-C S-glutathionylation with the regional strain in a model of doxorubicin-induced

cardiotoxicity (26). Several models of hypertension, familial hypertrophic myopathy, or exhausting exercise showed that S-glutathionylation of cMyBP-C slowed cross-bridge cycling kinetics and increased Ca^{2+}-sensitivity (20,21,27). In line with those findings, we found that cross-bridge-cycling kinetics during maximal Ca^{2+}-activation decreased in young GRMD dogs was reverted by ARM036. Interestingly, glutathione (GSH)-cMyBP-C was not detected in older GRMD dogs with HF, suggesting a transient mechanism occurring during early cardiac dysfunction (22).

Rycal compounds prevent RyR leak and intracellular Ca^{2+} overload in disease states. Most of the studies reporting improved cardiac muscle function with HF with Rycals have used mouse models (28,29). One study reported a protective effect of JTV-519-mediated RyR2 stabilization on HF using a dog model of rapid pacing (6). In our preclinical prospective study, ARM036 prevented the LV longitudinal strain decline and appearance of hypokinetic segments observed in placebo-treated GRMD dogs. By preventing LV function from degradation, ARM036 confirms the possibilities of this strategy in large animal models for other cardiac pathologies. The lack of effect of ARM036 on muscle function may be explained by the fact that at 2 months of age the skeletal muscle dysfunction is already profoundly established in GRMD dogs, which differs from the cardiac function at the same age. This raises the question of the therapeutic window. We reported recently that S107 in *mdx* mice was efficient only when administered early in very young animals (from 2 to 6 months of age) (30). A later therapy from 6 to 9 months of age, with more established cardiac dysfunction, had no major effect. Thus, ARM036 is specifically improving DMD-associated cardiomyopathy in our model. The global improvement of the muscular phenotype requires more experiments to find the best therapeutic windows, dose, and duration.

Previous studies have emphasized the pathophysiology of DMD skeletal muscle and heart, including the increased permeability of the cellular membrane, which resulted in increased intracellular Ca^{2+} leading to fibrosis, structural dysfunction, and impaired function. A recent study highlighted the perturbed expression of transcripts associated with fibrosis, reactive oxygen species, channels, and calcium signaling in DMD cardiomyopathy that were normalized in vitro after treatment with beta-blocker agents such as propranolol (31). The cardioprotective effect of ARM036 observed here was produced by restoring the normal FKBP12.6-mediated stabilization of the RyR2, preventing the Ca^{2+}-leak as indexed by the normalized RyR2 Po. Oxidative stress contributes to damages in Ca^{2+} handling and correlates with cardiomyopathy progression and the severity of HF in DMD patients (32). We and others have shown that restoring the redox balance reduces cMyBP-C S-glutathionylation (20,21,27). Although we did not directly assess oxidative stress, the prevention of cMyBP-C S-glutathionylation by ARM036 suggests that preventing Ca^{2+} leak may prevent oxidative stress (19). In the meantime, the ARM036 treatment in GRMD dogs normalized the cross-bridge cycling kinetics. This is consistent with a previous report showing that S-glutathionylation of cMyBP-C negatively affects cross-bridge cycling kinetics in mouse cardiomyocytes (33).

STUDY LIMITATIONS. This study may have limitations as the animals were only followed up until 6 months of age when mild LV dysfunction could be observed, and was designed to assess a preventive effect. Therefore, other studies should be designed to assess the potential curative effect of ARM036 treatment on longer period or initiated in the late stage where LV function is more severely altered.

CONCLUSIONS

Our major finding in this canine model of DMD is that chronic administration of ARM036 delayed the progression of LV dysfunction. Our results strongly suggest that such cardioprotective effect is produced by restoring the normal FKBP12.6-mediated stabilization and closed conformation of the RyR2 Ca^{2+} channel.

ACKNOWLEDGMENTS The authors thank the whole team of the BNMS Group 4 Lab animal facilities in EnvA for their daily cares of dogs.

FUNDING SUPPORT AND AUTHOR DISCLOSURES

This study was supported by the Association Française contre les Myopathies (AFM) (OC N°11590, AL N°15083, SB N° 14389, 15208, 15632, 16396, and 17124) and by Institut de Recherches Servier (Suresnes, France). The authors have reported that they have no relationships relevant to the contents of this paper to disclose.

ADDRESS FOR CORRESPONDENCE: Dr Olivier Cazorla, PhyMedExp, Université de Montpellier, INSERM, CNRS, CHU Arnaud de Villeneuve, 34295 Montpellier, France. E-mail: olivier.cazorla@inserm.fr. OR Dr Alain Lacampagne, PhyMedExp, Université de Montpellier, INSERM, CNRS, CHU Arnaud de Villeneuve, 34295 Montpellier, France. E-mail: alain.lacampagne@inserm.fr.

PERSPECTIVES

COMPETENCY IN MEDICAL KNOWLEDGE: DMD is associated with a cardiomyopathy. In a dog model, a phenotype of early cardiac dysfunction is caused by abnormal calcium handling and ameliorated by a calcium release channel stabilizer (Rycal).

TRANSLATIONAL OUTLOOK: Further investigations in patients with DMD are warranted to determine whether Rycal reduces or delays the development of cardiomyopathy and clarity the mechanisms involved.

REFERENCES

1. Emery AE. The muscular dystrophies. *Lancet*. 2002;359:687-695.

2. Nigro G, Comi LI, Politano L, Bain RJ. The incidence and evolution of cardiomyopathy in Duchenne muscular dystrophy. *Int J Cardiol*. 1990;26:271-277.

3. Porcher R, Desguerre I, Amthor H, et al. Association between prophylactic angiotensin-converting enzyme inhibitors and overall survival in Duchenne muscular dystrophy-analysis of registry data. *Eur Heart J*. 2021;42:1976-1984.

4. Bodensteiner JB, Engel AG. Intracellular calcium accumulation in Duchenne dystrophy and other myopathies: a study of 567,000 muscle fibers in 114 biopsies. *Neurology*. 1978;28:439-446.

5. Fauconnier J, Thireau J, Reiken S, et al. Leaky RyR2 trigger ventricular arrhythmias in Duchenne muscular dystrophy. *Proc Natl Acad Sci U S A*. 2010;107:1559-1564.

6. Yano M, Kobayashi S, Kohno M, et al. FKBP12.6-mediated stabilization of calcium-release channel (ryanodine receptor) as a novel therapeutic strategy against heart failure. *Circulation*. 2003;107:477-484.

7. Lehnart SE, Wehrens XH, Reiken S, et al. Phosphodiesterase 4D deficiency in the ryanodine-receptor complex promotes heart failure and arrhythmias. *Cell*. 2005;123:25-35.

8. Lehnart SE, Mongillo M, Bellinger A, et al. Leaky Ca2+ release channel/ryanodine receptor 2 causes seizures and sudden cardiac death in mice. *J Clin Invest*. 2008;118:2230-2245.

9. Franco A Jr, Lansman JB. Calcium entry through stretch-inactivated ion channels in mdx myotubes. *Nature*. 1990;344:670-673.

10. Cooper BJ, Winand NJ, Stedman H, et al. The homologue of the Duchenne locus is defective in X-linked muscular dystrophy of dogs. *Nature*. 1988;334:154-156.

11. Su JB, Cazorla O, Blot S, et al. Bradykinin restores left ventricular function, sarcomeric protein phosphorylation, and e/nNOS levels in dogs with Duchenne muscular dystrophy cardiomyopathy. *Cardiovasc Res*. 2012;95:86-96.

12. Chetboul V, Escriou C, Tessier D, et al. Tissue Doppler imaging detects early asymptomatic myocardial abnormalities in a dog model of Duchenne's cardiomyopathy. *Eur Heart J*. 2004;25:1934-1939.

13. Amedro P, Vincenti M, De La Villeon G, et al. Speckle-tracking echocardiography in children with Duchenne muscular dystrophy: a prospective multicenter controlled cross-sectional study. *J Am Soc Echocardiogr*. 2019;32:412-422.

14. Ghaleh B, Barthelemy I, Sambin L, et al. Alteration in left ventricular contractile function develops in puppies with Duchenne muscular dystrophy. *J Am Soc Echocardiogr*. 2020;33:120-129.

15. Jozwiak M, Meli AC, Melka J, et al. Concomitant systolic and diastolic alterations during chronic hypertension in pig. *J Mol Cell Cardiol*. 2019;131:155-163.

16. Ait Mou Y, Reboul C, Andre L, Lacampagne A, Cazorla O. Late exercise training improves non-uniformity of transmural myocardial function in rats with ischaemic heart failure. *Cardiovasc Res*. 2009;81:555-564.

17. Johnston AS, Lehnart SE, Burgoyne JR. Ca(2+) signaling in the myocardium by (redox) regulation of PKA/CaMKII. *Front Pharmacol*. 2015;6:166.

18. Cazorla O, Szilagyi S, Vignier N, et al. Length and protein kinase A modulations of myocytes in cardiac myosin binding protein C-deficient mice. *Cardiovasc Res*. 2006;69:370-380.

19. Xiong Y, Uys JD, Tew KD, Townsend DM, S-glutathionylation. from molecular mechanisms to health outcomes. *Antioxid Redox Signal*. 2011;15:233-270.

20. Chakouri N, Reboul C, Boulghobra D, et al. Stress-induced protein S-glutathionylation and phosphorylation crosstalk in cardiac sarcomeric proteins – impact on heart function. *Int J Cardiol*. 2018;258:207-216.

21. Wilder T, Ryba DM, Wieczorek DF, Wolska BM, Solaro RJ. N-acetylcysteine reverses diastolic dysfunction and hypertrophy in familial hypertrophic cardiomyopathy. *Am J Physiol Heart Circ Physiol*. 2015;309:H1720-H1730.

22. Ait Mou Y, Lacampagne A, Irving T, et al. Altered myofilament structure and function in dogs with Duchenne muscular dystrophy cardiomyopathy. *J Mol Cell Cardiol*. 2018;114:345-353.

23. Ait Mou Y, Toth A, Cassan C, et al. Beneficial effects of SR33805 in failing myocardium. *Cardiovasc Res*. 2011;91:412-419.

24. Derumeaux G, Ovize M, Loufoua J, Pontier G, Andre-Fouet X, Cribier A. Assessment of nonuniformity of transmural myocardial velocities by color-coded tissue Doppler imaging: characterization of normal, ischemic, and stunned myocardium. *Circulation*. 2000;101:1390-1395.

25. Hamdani N, Bishu KG, von Frieling-Salewsky M, Redfield MM, Linke WA. Deranged myofilament phosphorylation and function in experimental heart failure with preserved ejection fraction. *Cardiovasc Res*. 2013;97:464-471.

26. Chakouri N, Farah C, Matecki S, et al. Screening for in vivo regional contractile defaults to predict the delayed doxorubicin cardiotoxicity in juvenile rat. *Theranostics*. 2020;10:8130-8142.

27. Jeong EM, Monasky MM, Gu L, et al. Tetrahydrobiopterin improves diastolic dysfunction by reversing changes in myofilament properties. *J Mol Cell Cardiol*. 2013;56:44-54.

28. Wehrens XH, Lehnart SE, Huang F, et al. FKBP12.6 deficiency and defective calcium release channel (ryanodine receptor) function linked to exercise-induced sudden cardiac death. *Cell*. 2003;113:829-840.

29. Wehrens XH, Lehnart SE, Reiken SR, et al. Protection from cardiac arrhythmia through ryanodine receptor-stabilizing protein calstabin2. *Science*. 2004;304:292-296.

30. Vincenti M, Farah C, Amedro P, Scheuermann V, Lacampagne A, Cazorla O. Early myocardial dysfunction and benefits of cardiac treatment in young X-linked Duchenne muscular dystrophy mice. *Cardiovasc Drugs Ther*. Published

online June 17, 2021. https://doi.org/https://link.springer.com/article/10.1007%2Fs10557-021-07218-7

31. Kamdar F, Das S, Gong W, et al. Stem cell-derived cardiomyocytes and beta-adrenergic receptor blockade in Duchenne muscular dystrophy cardiomyopathy. *J Am Coll Cardiol*. 2020;75:1159-1174.

32. Law ML, Cohen H, Martin AA, Angulski ABB, Metzger JM. Dysregulation of calcium handling in Duchenne muscular dystrophy-associated dilated cardiomyopathy: mechanisms and experimental therapeutic strategies. *J Clin Med*. 2020;9.

33. Stathopoulou K, Wittig I, Heidler J, et al. S-glutathiolation impairs phosphoregulation and function of cardiac myosin-binding protein C in human heart failure. *FASEB J*. 2016;30:1849-1864.

KEY WORDS contractile proteins, heart failure, left ventricular dysfunction, length dependent activation, myofilament properties, transmural heterogeneity